JOURNAL OF MATERIALS SCIENCE 11 (1976) 1857–1866

Mechanical properties of molybdenum-sealing glass-ceramics

J. C. SWEARENGEN, R. J. EAGAN
Sandia Laboratories, Albuquerque, New Mexico, USA

Elastic constants, thermal expansion, strength, and fracture toughness were determined for a glass-ceramic which bonds to molybdenum and matches its thermal expansion. Mechanical properties of the glass-ceramic were related to microstructure following two different crystallization treatments and moderate changes in composition. Crystallization increases the toughness and modulus of the parent glass even while the residual glass properties decline. Fracture toughness of the composite is shown to depend primarily upon properties of the separate phases; however, internal stresses are shown to decrease toughness without decreasing Young's modulus.

1. Introduction

Several benefits may be realized if conventional ceramics in high-temperature vacuum tubes can be replaced by a glass-ceramic which bonds directly to metal components. For example, glass-ceramics are formed as glass, so that grinding of tube envelopes becomes unnecessary. Direct bonding to metal can eliminate metallize/braze operations; furthermore, thermal expansion of the glass-ceramic can be adjusted so that residual stresses at joints can be reduced. Glass-ceramics which incorporate zinc–silicate as the crystal phase can be bonded successfully to molybdenum. Accordingly, a study was required to evaluate these materials for potential use as vacuum tube insulators. It was necessary to determine the effect of processing variables on the mechanical and physical properties relevant to tube design, and to relate these properties to microstructure.

The mechanical properties of glass-ceramics are often superior to those of the glasses from which they are formed. Elastic moduli are increased by precipitation of more rigid crystalline phases, and strength and/or fracture toughness is improved whenever the presence of the crystals produces increased resistance to fracture propagation. Since glass-ceramics are composed of a dispersion of hard crystals within a glass matrix, it would be expected that the elastic properties, and possibly strengths, could be predicted by the relations of mixture theory. Freiman and Hench [1] compared theoretical predictions with measurements of Young's modulus and thermal expansion coefficient for a stoichiometric $Li_2O·2SiO_2$ glass-ceramic crystallized to various extents. They found reasonable agreement with predictions for this material in which residual glass composition remained constant during crystallization. Strength enhancement in the $Li_2O·2SiO_2$ glass-ceramic was attributed to a decrease in the mean free path between crystals during crystallization, but an eventual reduction in strength occurred if microcracks developed at the glass–crystal interfaces due to volume changes during crystallization. The observation concerning microcracks may relate to an earlier one by Watanabe *et al.* [2] wherein if care was taken to avoid surface damage to the parent glass, the effect of crystallization was to reduce strength rather than increase it. Similarly, Borom *et al.* [3] found that lithium disilicate glass-ceramics crystallized below 800° C exhibited strengths no higher than that of the abraded parent glass, and in fact a reduction in strength occurred due to loss of coherency between glass and crystal.

Hasselman and Fulrath [4, 5] studied the effects of particle size and volume fraction of crystal phase on the strength of a glass–crystal composite free of internal stresses. They hypothesized that the role of dispersions in increasing fracture strength is to limit the maximum flaw size to the interparticle spacing. In that case, the strength should be independent of the crystalline dispersion at low volume fractions, but depend on both volume fraction and crystal size at high volume fractions. On the other hand, Frey and Mackenzie [6] concluded that dispersions of Al_2O_3 or ZrO_2 in a glass matrix increase the strength in direct proportion to the concurrent increase in composite elastic moduli. Miyata and Jinno [7] re-analysed the data of Hasselman and Fulrath [4] and concluded that at low volume fractions, composite strength may decrease with increasing fractions of crystal phase. They attributed this behaviour to the effect of "pre-existing structural imperfections" near the glass–crystal interfaces. Neither the explanation by Hasselman and Fulrath [4, 5] nor Miyata and Jinno [7] are in accord with the observations of Freiman and Hence [1], possibly because of the existence of the microcracks that are postulated by the latter.

Fracture toughness of a glass-ceramic can be enhanced over that of the parent glass if the crystals cause an increase in the fracture surface area. The interphase stresses that may arise during crystallization are of major importance in determining the fracture propagation path. These may arise from volume changes, as Freiman and Hench [1] suggested, or they may arise from differential contraction during cooling. For the case where the thermal expansion of the crystal is lower than that of the glass, circumferential tensile stresses (and microcracks) may develop in the glass phase together with radial compressive stresses at the glass–crystal interfaces. Fracture in systems of this type tends to propagate through the crystals. The increase in toughness by this mechanism is usually less than in systems where the crystal contracts more than the glass. In the latter case the fracture path tends to deviate around the crystals or follow the glass–crystal interfaces [8].

TABLE I Composition (wt%) of materials under study

	NK2/ 2228	MS 011	MS 011 residual glass A	MS 39	MS 44
SiO_2	47.4	46.4	61.7	39.0	39.0
ZnO	32.2	32.2		44.5	45.0
Al_2O_3	9.5	9.5	17.0	8.0	7.0
Nucleating agents and modifiers (proprietary)	10.9	11.9	21.3	8.5	9.0

In what follows we describe techniques for preparation and testing of zinc–silicate glass-ceramics. Measured mechanical properties are related to microstructure, and the relationships thereby identified are discussed in light of concepts taken from the literature.

2. Experimental procedure

The approximate compositions of Mexim NK2/2228* and MS 011 glass-ceramics are displayed in Table I. For proprietary reasons, unfortunately, we are unable to list the detailed compositions of these two systems. The composition of the residual glass in MS 011 is based upon the assumption that all the ZnO in the parent glass was incorporated into the crystal phase, i.e. Zn_2SiO_4. The validity of this assumption will be analysed later. The primary purpose of this study was to understand the behaviour of Mexim NK2/2228 and MS 011 glass-ceramics. Modified compositions were produced and evaluated, however, with the constraint that each glass-ceramic must seal to molybdenum and match its thermal expansion from room temperature to the sealing temperature. Compositions MS 39 and 44 have more ZnO, and hence more crystalline phase than the NK2/2228 and MS 011 systems.

2.2. Material preparation

Each batch of glass was prepared by fusing reagent-grade chemicals in a platinum crucible. The glass was melted and maintained for 24 h at 1500 to 1600° C in an electric furnace; to ensure homogeneity the melt was stirred continuously for 18 h. The molten glass was then cast onto a heated steel plate coated with graphite powder, and quickly transferred to an annealing oven preheated to 610° C. The temperature was maintained for 5 min and then reduced at the rate of $0.4° C min^{-1}$ to produce the annealed glass.

Crystallization of the glass is accomplished by thermal treatment. In the production of vacuum tube envelopes, crystallization is accomplished simultaneously with the sealing to molybdenum during a temperature cycle similar to that labelled "1050° seal" in Fig. 1. Accordingly, glass-ceramics for mechanical testing were produced by this cycle. For purposes of comparison the 650/950° C

---

*English Electric Co, Ltd.

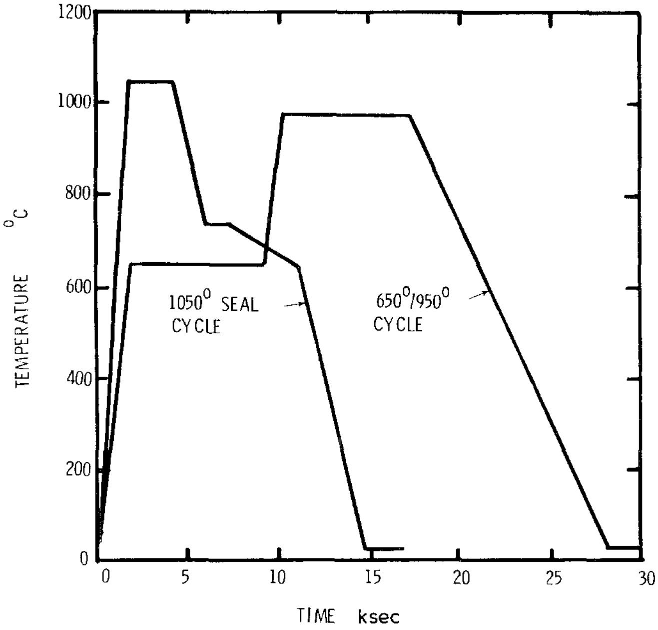

Figure 1 Thermal excursions employed in crystallization/sealing of MS 011.

cycle was also utilized (Fig. 1). In the latter case, nucleation occurs at the lower temperature and a finer dispersion of crystal phase is produced. For either thermal cycle, the cooling rate is slow enough to ensure that annealing of the matrix glass is complete. Samples of the residual glass were prepared by the same techniques used for the parent glass. Zinc orthosilicate samples were prepared by fusing a stoichiometric mixture of ZnO and SiO_2. Upon slow cooling, the melt crystallized to produce fine-grained polycrystalline Zn_2SiO_4 (willemite).

2.2. Characterization

X-ray diffraction techniques were utilized to identify the crystalline phase. The only crystalline phase ever detected for any of the systems in Table I was willemite, Zn_2SiO_4. The microstructures of the glasses and glass-ceramics were studied via scanning electron microscopy of polished and etched sections (15 sec in 2% HF). Fracture surface morphology was studied via transmission electron microscopy of gold-shadowed carbon replicas. The density of each material was determined from liquid displacement measurements, employing Freon TF as the medium. Thermal expansion behaviour was measured using a dual push-rod dilatometer.† The glass transition temperature was determined by extrapolating linear portions of the expansion curve to the point of intersection. The transition temperature results from the onset of structural relaxation as the glass passes into the supercooled liquid regime upon heating, or the reverse on cooling, and is reproducible.

Young's moduli, shear moduli, and Poisson's ratio were measured ultrasonically, using the pulse-overlap technique. Fracture strengths were determined from four-point bend tests of rectangular beams, approximately 80 mm x 4 x 10 mm in size. The beam surfaces were as diamond-sawed, with the edges chamfered. More consistent strength measurements would likely result from testing cylindrical bars, but we do not at present have the capability of fabricating rod-shaped samples.

Fracture toughness, K_{IC} was determined from three-point bend tests of notched and thermally-precracked beams. The beams were sized to yield a span-to-width ratio of about 4 and beam thicknesses were 1.3 to 4.0 mm. The variation in thickness was purposely introduced to ensure that measured K_{IC} values were independent of free surface effects. A small notch was diamond-sawed in one edge of each beam and a stable precrack was induced to propagate from the notch by application of a solder gun tip to the material surface just ahead of the notch. Precrack lengths could be unambiguously determined by observation of the fracture surfaces under low magnification. Fracture toughness (K_{IC}) values were calculated from method of Brown and Srawley [9].

In contrast to the stoichiometric glass-ceramic studied by Freiman and Hench [1], the com-

---

† Dilatronic IX, Theta Industries, Port Washington, New York, USA.

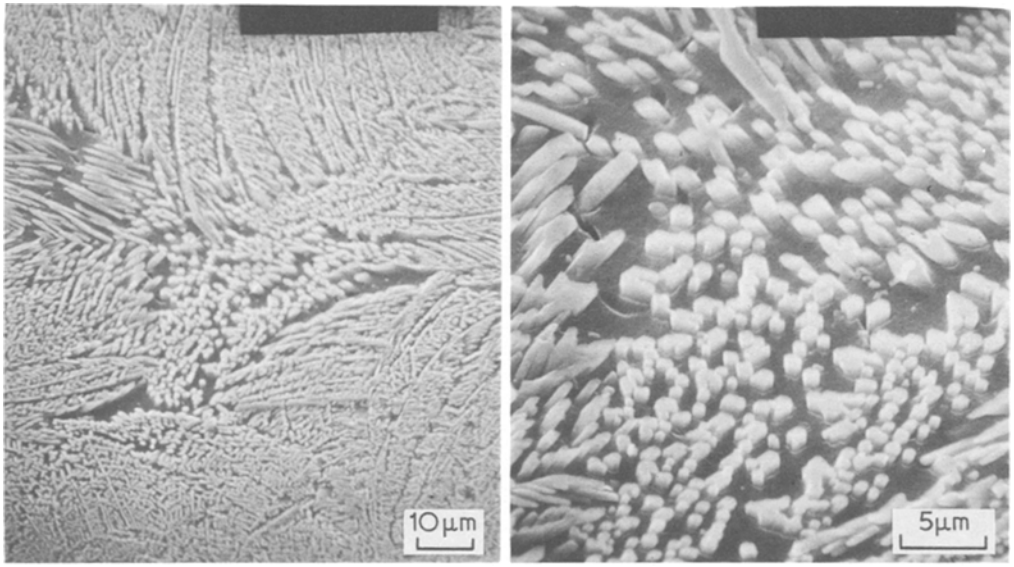

Figure 2 Microstructure of MS 011 (1050° C seal cycle). Sections polished and etched in HF (General Electric Company, St. Petersburg, FL).

position of the residual glass in these glass-ceramics is changed by the crystallization treatments. For micromechanical characterization of the materials in the present study, the properties of each phase must be determined separately. Most of the characterization steps described above were applied sequentially to the annealed parent glass, the crystallized glass-ceramic, the residual glass, and the polycrystalline samples of Zn_2SiO_4.

3. Results

3.1. Mechanical properties

If all the ZnO crystallizes to form Zn_2SiO_4, the parent glass will transform to a two-phase structure consisting of 31.3 vol % crystal phase dispersed in a matrix of residual glass. Although the chemistry of the glass is complex (Table I), the microstructure of the glass-ceramic consists of two homogeneous phases. The microstructure produced by the 1050° C seal cycle is displayed in Fig. 2; lower magnification photos would reveal the spherulitic morphology of the crystalline phase.

The density (ρ), average fracture strength ($\bar{\sigma}_f$), thermal expansion coefficient from 23 to 600° C (α), Young's modulus (E), and fracture toughness (K_{IC}) for Mexim and MS 011 are summarized in Table II. It is apparent that the 650/950° C cycle changes these properties but little from the 1050° C cycle. Likewise, some properties of the modified glass-ceramics are also listed. (For purposes of comparison, α for molybdenum is $55 \times 10^{-7}\,{}^\circ C^{-1}$.) The data in Table II indicate that the modified compositions develop higher moduli than

TABLE II Mechanical and physical properties of molybdenum-sealing glass-ceramics (compositions given in Table I)

Material	Thermal treatment	ρ(g cm^{-3})	$\bar{\sigma}_f$(MPa)	α(10^{-7}° C^{-1})	E(GPa)	K_{IC}(MN m$^{-3/2}$)	T_g(°C)
NK2/2228	1050° C	3.045	89.6	49.0	81	1.11 ± 0.1	737
	650/950° C	3.035	102.0	48.2	80.5		
MS 011	1050° C	3.033	82.7	51.8	80.8	1.03 ± 0.05	737
	650/950° C	3.033	92.4	50.7	79.1	0.90	
MS 011	Glass	3.038	83.4	59.0	81.8	0.87 ± 0.03	
MS 011	Residual glass "A"	2.477		62.4	76.6	0.73 ± 0.08	740
Zn_2SiO_4	Polycrystal	4.27		24.0	96.5		
MS 39	1050° C	3.240	93.1	50.7	83.8	0.85 ± 0.01	705
MS 44	1050° C	3.352	102.0	53.0	87.9	0.94 ± 0.2	695

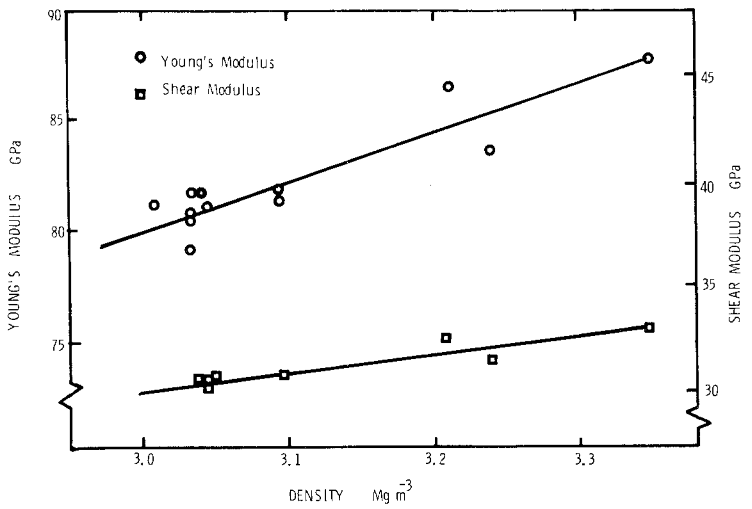

Figure 3 Young's and shear moduli versus density for zinc–silicate glass-ceramics.

NK2/2228 and MS 011 without a corresponding uniform increase in toughness. This behaviour is a result of the two-phase nature of the systems, as will be discussed later. Young's moduli and shear moduli for all the glass-ceramics tested are plotted as functions of ρ in Fig. 3; a monotonic rise in moduli with density is observed. No dependence of elastic moduli upon orientation was observed; that is, the materials can be considered isotropic.

For NK2/2228 and MS011 the values of K_{IC} show a monotonic rise with Young's modulus, as displayed in Fig. 4. The trend is clear even though two crystallization treatments and two slightly different compositions are plotted. Interestingly, but perhaps fortuitously, the toughness of MS 011 residual glass falls on the same curve. Values of K_{IC} for the denser group of materials, MS 39 and 44, also increase with E; but the 39-44 system falls on a different curve. The toughness of uncrystallized MS 011 glass is displayed for comparison. The fracture strengths do not have the same trend as the toughness; however, measured fracture strengths were subject to considerable scatter and since the $\bar{\sigma}_{\text{f}}$ values are determined from three or four tests, it should not be concluded that no such correlation exists.

The relatively low values of K_{IC} in these glass-ceramics and the increase in K_{IC} with E both indicate that the fracture path is not deflected greatly by the crystals, and that microcracks do not develop within the matrix glass during crystallization. This conclusion is supported by the

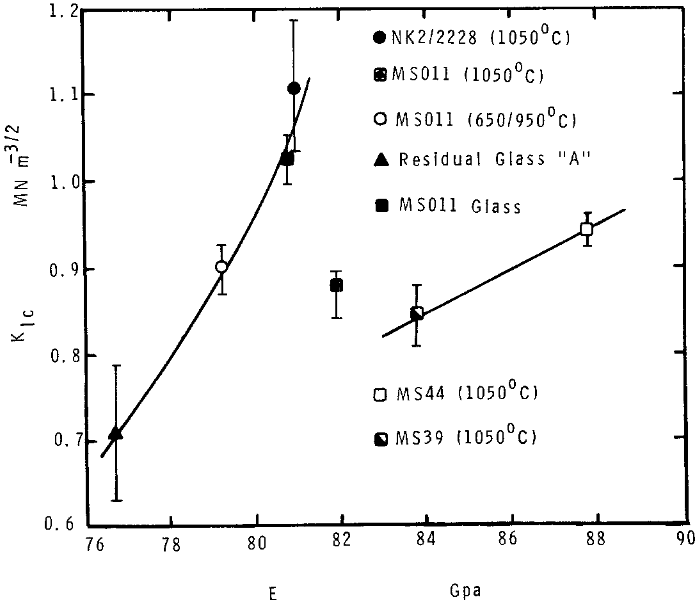

Figure 4 Fracture toughness (K_{IC}) versus Young's modulus for molybdenum-sealing glass-ceramics.

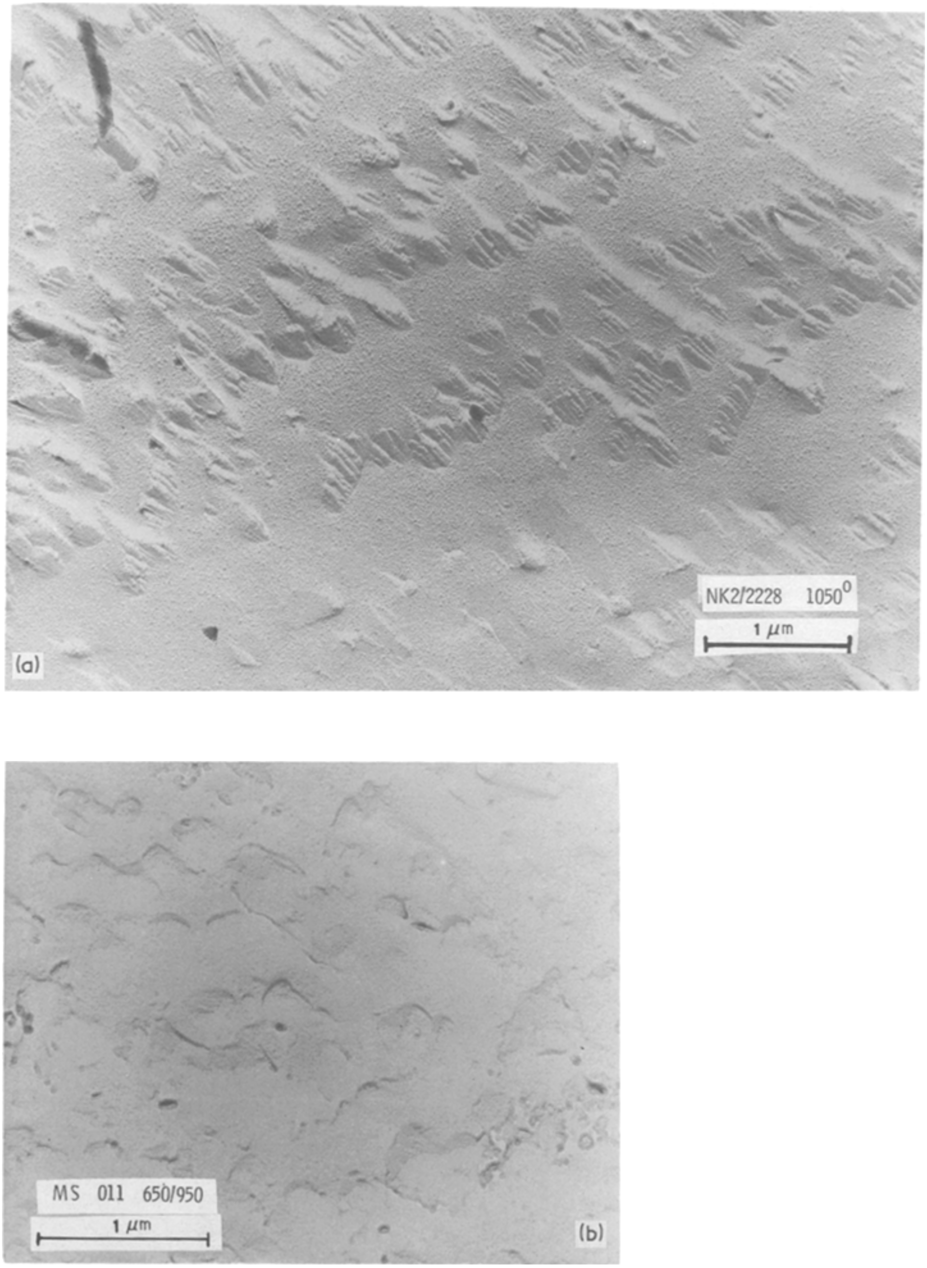

Figure 5 Gold-shadowed carbon replica of fracture surface. (a) Mexim NK2/2228, 1050° C seal cycle; (b) MS 011, 650/950° C seal cycle; (c) MS 39, 1050° C seal cycle.

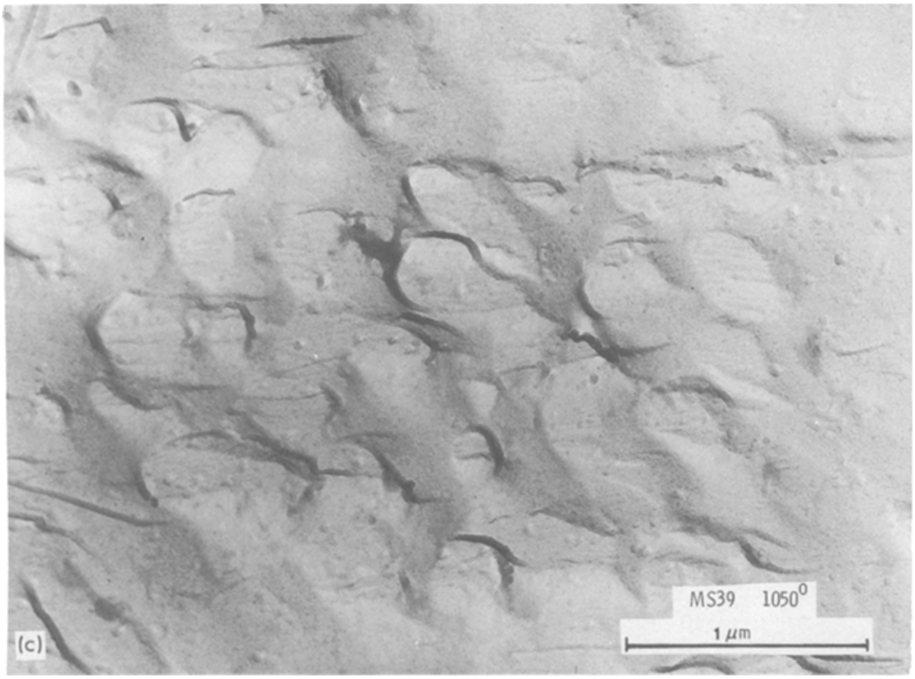

Figure 5 continued.

fractographs of Fig. 5a to c, wherein the crystals can be identified on the fracture surface. Note the apparent cleavage facets on the fracture surfaces within the crystals. The lower toughness produced by the 650/950° C cycle in MS 011 (Table II) is corroborated by the appearance of the fracture surface, Fig. 5b. The finer crystal dispersion produces less fracture path deviation and thus lower K_{IC}. The fracture surface of MS 011 parent glass is displayed in Fig. 6; the crystal phase is not in evidence, as expected.

3.2. Mixture theory applied to MS 011

In the absence of porosity, the density of the glass-crystal composite will be given simply by the sum of the fractional densities, i.e.

$$\rho = \rho_1 V_1 + \rho_2 V_2 , \tag{1}$$

where the subscripts 1 and 2 refer to crystal and residual glass phases, respectively, and V is the volume fraction of a component. If each phase is treated as isotropic (this is, of course, an approximation for the dispersed Zn_2SiO_4 crystals, which have the rombohedral structure), a simple lower bound to composite Young's modulus is given by

$$E = E_1 V_1 + E_2 V_2 \tag{2}$$

Because Equation 2 is one-dimensional in nature, it requires the two phases to have equal Poisson's ratios and to undergo equal strains; the relation is also limited to situations where E_1 and E_2 do not differ by more than a factor of about two. More precise bounds have been constructed which take into account the differences in Poisson's ratios and/or bulk moduli [10], but in view of the approximations involved in application to these glass-ceramics, Equation 2 is considered to present an adequate estimate for composite Young's modulus.

Likewise, composite thermal expansion can be predicted in approximate [11] and more exact [12] fashions. Either approach requires assumptions concerning the geometry of the dispersed phase which are not appropriate to these glass-ceramics; nevertheless, some insights into composite behaviour can be gained from the computation. If each dispersed particle is treated as an elastic sphere imbedded in an infinite elastic continuum, a symmetrical stress distribution results and composite expansion becomes [12]

$$\alpha = \alpha_2 - V_1 A(\alpha_2 - \alpha_1) \tag{3}$$

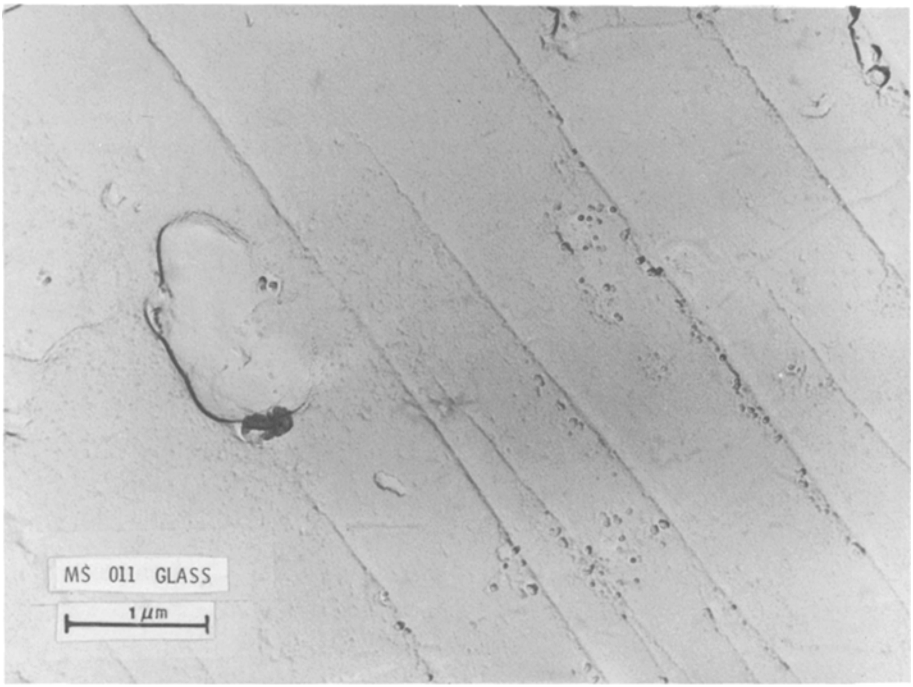

Figure 6 Gold-shadowed carbon replica of fracture surface: MS 011, parent glass.

where

$$A = \frac{(1+\nu_2)/2E_2}{[(1+\nu_2)/2E_2] + [(1-2\nu_1)/E_1]}$$

and ν is Poisson's ratio. The relation is restricted to temperature intervals over which the α_i are linear.

In order to apply Equations 1 to 3 to predictions of MS 011 properties, the required properties of each phase must be determined. Two different residual glasses were produced: glass "A", which has no ZnO present (corresponding to the situation where all the Zn_2SiO_4 is crystallized) and glass "C", representative of the situation where 5% of the Zn_2SiO_4 remained in solution. The thermal expansion behaviour of the glass-ceramic, crystal, and both residual glasses is shown in Fig. 7.

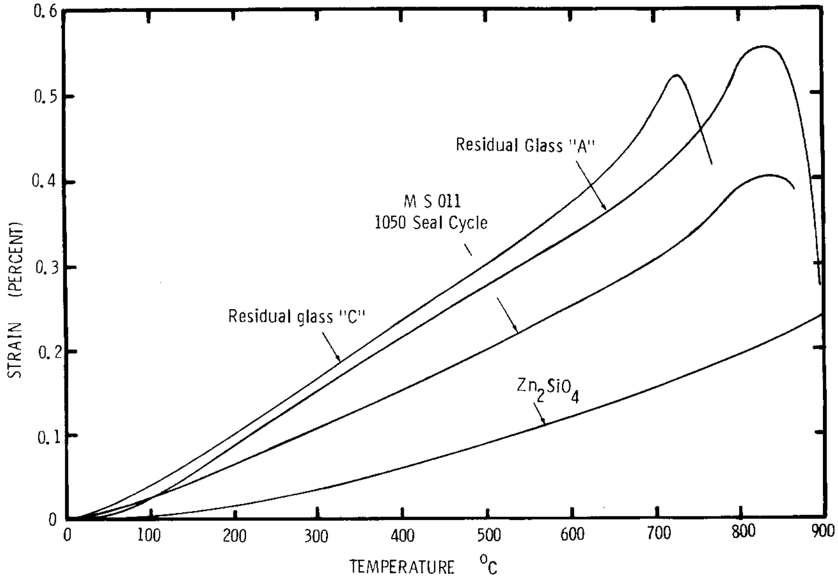

Figure 7 Thermal expansion behaviour of MS 011 (1050° C seal cycle) and its constituents. T_g of glass A, MS 011 and glass C are 740, 737 and 670° C, respectively.

The glass-transition behaviour in the glass-ceramic results entirely from transition behaviour of the residual glass [13], and only glass "A" has a transition temperature corresponding to that of the composite. Because T_g is manifested by a change in enthalpy of the glass, DTA results can be employed to compare T_g of residual glass and glass-ceramic. The DTA and dilatometric results are in complete agreement. The coincident values of T_g for glass "A" and MS 011 indicates that crystallization was complete. Accordingly, glass composition "A" was used for residual glass properties (Table I).

Modulus and density values for use in Equations 1 and 2 were taken from Table II. The coefficients of thermal expansion for Equation 3 were taken from Fig. 7, averaged over the temperature interval (25 to 600° C) where the behaviour is nearly linear. Values of E, α, and ρ for the crystal, residual glass "A", and glass-ceramic are displayed in Table III, along with glass-ceramic properties predicted using Equations 1 to 3. Poisson's ratio for the crystal and residual glass, as required by Equation 3, were determined by the pulse-overlap technique to be 0.36 and 0.205, respectively. Agreement between theory and experiment is considered to be quite satisfactory in view of the geometric approximations involved.

4. Discussion

A comparison of K_{IC} results in this study with representative values from the literature is given in Table IV. The fracture toughness of MS 011 residual glass corresponds closely to that determined for 96% silica and fused silica glasses. The toughness of the NK2/2228 and MS 011 glass-ceramics is slightly less than that of Corning 0337 [19], a glass-ceramic having greater than 60 vol % crystal phase. The toughness is also considerably below that for polycrystalline ceramics, as exemplified by 96% alumina and Lucalox. These results are in accord with observations of the microstructure and fracture morphologies of the molybdenum-sealing glass-ceramics.

TABLE III Application of mixture theory to MS 011 (1050° C seal cycle)

	Zn_2SiO_4	Residual glass "A"	31.3% composite (1050° C seal)
E(GPa)	96	76.6	Predicted 83.9 Measured 80.8
α(10^{-7}° C^{-1}, 25 to 600° C)	22.1	59.7	Predicted 50.8 Measured 45.0
ρ(g cm^{-3})	4.27	2.477	Predicted 3.034 Measured 3.033

The success of mixture theory in predicting composite modulus and thermal expansion indicates that MS 011 glass-ceramic is sufficiently continuous on the microscale to transfer loads between the phases. The fracture toughness data support the same contention; that is, since K_{IC} increases approximately in proportion to $(E\gamma)^{1/2}$ and surface energy (γ) is known to increase with Young's modulus [14], it is likely that K_{IC} will increase with E, as shown in Fig. 4. A similar trend was observed for the modified system as well. The anticipated relation between K_{IC} and E really applies only to a single-phase material free of flaws or microstresses, whereas the effective surface energy (or K_{IC}) of a two-phase material is more easily measured than predicted. In fact, in the presence of a second phase or microcracks, K_{IC} may sometimes decrease, as E increases [15]. The correlation displayed in Fig. 4 is in accord with the relation between strength and modulus observed by Frey and Mackenzie [6]. The results indicate that the toughness is controlled primarily by changes in effective γ, and not by the effect of dispersions on flaw size [4, 5].

Compositions MS 39 and 44 have more of the low-expansion Zn_2SiO_4 phase than do NK2/2228 and MS011. In order to maintain thermal expansion match with molybdenum, the expansion coefficient of the matrix glass in MS 39 and 44 must be increased. An unavoidable side effect of these changes is that internal stresses will increase, and K_{IC} will decrease compared to the NK2/2228 and

TABLE IV Comparative values for K_{IC} for glasses, ceramics, and glass-ceramics

Material	K_{IC}(MN m$^{-3/2}$)	Reference
Al_2O_3/4% MgO	4.6	[16]
Lucalox	4.1	[16]
Corning 0337 glass-ceramic	1.5	[19]
Electrical porcelain	1.1	[17]
MS 011	1.0	This study
Fused silica	0.75	[18]
MS 011 residual glass	0.73	This study
96% Silica	0.71	[18]

MS 011 materials. In addition to matching thermal expansion, the optimum ceramic for joining to metals would have high toughness and low modulus. In the light of these objectives, the data in Fig. 4 indicate that the modifications introduced to produce MS 39 and 44 were deleterious, and the MS 011-NK2/2228 system remains the system of choice for sealing to molybdenum. Composition MS 011 is a somewhat better choice than NK2/2228, because its thermal expansion is more closely matched to that of molybdenum.

The beneficial effect on toughness of adding crystals to a glass must be discerned by comparing K_{IC} of the glass-crystal composite to that of the parent glass *and* the residual glass. For the MS 011 glass-ceramic, the composite toughness is increased about 15% over that of the parent glass and about 50% over that of the residual glass. The formation of the crystalline phase increases the composite toughness, but that increase is offset somewhat by a decrease in toughness of the residual glass.

The absence of microcracking as a controlling parameter on toughness in these systems in indicated by the transgranular fracture observed in Fig. 5, and by the fact that K_{IC} increases with Young's modulus. Additional support for this conconclusion in MS 011 is drawn from the fact (Table II) that K_{IC} is not improved by the 650/950° C nucleation/growth cycle in comparison to the 1050° C cycle, even though the crystals are more uniform and smaller. It appears likely, then, that the toughness of these molybdenum-sealing glass-ceramics is controlled by fractional contributions from each phase, but internal stresses due to thermal expansion differences can have a significant effect on the composite properties.

5. Conclusions

A dispersion of Zn_2SiO_4 crystals in the matrix glass of these molybdenum-sealing glass-ceramics can produce composite properties that are superior to those of the parent glass or the matrix glass. The beneficial effects produced by partial crystallization of the parent glass can be offset somewhat by declines in the properties of the matrix glass.

Some of the mechanical properties of these materials can be predicted from the properties of the component phases by using the appropriate mixture relations. The composite fracture toughness is determined primarily by the toughnesses of the phases; however, interactive effects such as internal stresses or microcracking can reduce the toughness without decreasing Young's modulus.

Acknowledgements

The authors thank J. Mata, R. D. Bland, J. A. Gilbert, H. J. Gregory, J. Gieske, and C. R. Hills for their contributions to the experimental portions of this programme, and they would like to acknowledge the many helpful discussions with E. K. Beauchamp during the course of the study. This work was supported by the US Energy Research and Development Administration.

References

1. S. W. FREIMAN and L. L. HENCH, *J. Amer. Ceram. Soc.* **55** (2) (1972) 86.
2. M. WATANABE, R. V. CAPORALI, and R. E. MOLD, "Symposium on Nucleation and Crystallization of Glasses", edited by M. K. Reser (American Ceramic Society, Columbus, Ohio, 1962) pp. 23–28.
3. M. P. BOROM, A. M. TURKALO, and R. H. DOREMUS, *J. Amer. Ceram. Soc.* 58 (9–10) (1975) 385.
4. D. P. H. HASSELMAN and R. M. FULRATH, *ibid* **49** (2) (1966) 68.
5. *Idem, ibid* **50** (8) (1967) 399.
6. W. J. FREY and J. D. MACKENZIE, *J. Mater. Sci.* **2** (1967) 124.
7. N. MIYATA and H. JINNO, *ibid* 7 (1972) 973.
8. P. W. MCMILLAN, "Glass Ceramics" (Academic Press, London, 1964).
9. W. F. BROWN, JUN. and JOHN E. SRAWLEY, ASTM STP 140, Am. Soc. for Test. & Mater. (1966).
10. Z. HASHIN and S. SHTRIKMAN, *J. Mech. Phys. Soc.* **11** (1963) 127.
11. W. D. KINGERY, "Introduction to Ceramics", (Wiley, New York, 1960).
12. R. R. TUMMALA and A. L. FRIEDBERG, *J. Appl. Phys.* **41** (1970) 5104.
13. ARNOLD BONDI, "Physical Properties of Molecular Crystals, Liquids, and Glasses", (Wiley, New York, 1968) p. 381.
14. J. J. DUGA, DCIC Report 69-2, Battelle Columbus Laboratories (1969).
15. N. CLAUSSEN, Paper 60-B-75, presented at 77th Meeting of American Ceramic Society, Washington, DC, 3–8 May (1975).
16. R. F. PABST, in "Fracture Mechanics of Ceramics", Vol. 2, edited by R. C. Bradt, D. P. H. Hasselman, and F. F. Lange (Plenum Press, New York, 1974) pp. 555-565.
17. W. G. CLARK, JUN. and W. A. LOGDSON, *ibid*, pp. 843–861.
18. S. M. WIEDERHORN, *ibid*, pp. 829–841.
19. E. K. BEAUCHAMP, Sandia Laboratories Report SAND-75-0273 (July 1975).

Received 20 February and accepted 19 March 1976.